Damage Detection and Identification of Smart Composites Using Optical Fiber Sensors

Chang-Sun Hong and Hyung-Joon Bang
Aerospace Engineering Division, Korea Advanced Institute of Science and Technology
Taejon, 305-701, Korea

Abstract: The objective of this study is to develop simultaneous failure detection and strain measurement techniques of composite materials in real-time using optical fiber sensors. To detect the failure signal, extrinsic Fabry-Perot interferometer (EFPI) system using laser diode(LD) was used and absolute EFPI (AEFPI) system with ASE broadband source was implemented for the strain measurement. Signals due to matrix crack and fiber breakage in composite laminates were treated by a signal processing program in real-time. This paper describes the application of time-frequency analysis such as Short Time Fourier Transform (STFT) and Wavelet Transform (WT) to identify the moment of failure. The ASE source and LD were applied in a single EFPI sensor using a wavelength division multiplexer(WDM) to monitor strain and failure simultaneously. From the result of the tensile test, strain measured by the AEFPI agreed with the value of electric strain gage and the failure detection system could detect the moment of failure with high sensitivity to recognize the onset of micro-crack failure signal.

Key words: *Optical Fiber Sensor, Smart Composites, Damage Detection , Health Monitoring*

1. INTRODUCTION

Composite materials have been used in the wide fields of aerospace and other industries. Composites can exhibit surprising performance but the structural damages by external effects such as excessive load and impact load can degrade the integrity of the composite structures. Therefore, it is desirable to establish new non-destructive evaluation (NDE) techniques for in-service monitoring of composite structures to guarantee the structural safety. Experiments are indispensable for understanding and predicting the behavior and failure of a wide variety of composite materials.

In recent years, a lot of attention has been paid to the optical fiber sensors for smart materials and structures. The use of this dielectric sensor is preferable for embedding in composite materials, and optical fibers possess many other advantages which render them suitable for this purpose. Fiber optic sensors can make useful measurements of a structure's state of strain, temperature, and vibration[1-4]. And they can also be used to predict the onset of structural failure, thereby allowing timely preventive measures to be taken[5-7]. EFPI has good sensitivity to detect the stress waves from structural failure[4] and AEFPI which uses broad band light source can measure the strain without accumulation of errors[2]. This paper will focus on the simultaneous sensing of strain and failure signals in composite laminates using an EFPI sensor. And the characteristics of stress wave signals from composites failure will be discussed.

2. FIBER OPTIC SENSOR

2.1. EFPI for stress wave detection

Fabry-Perot interferometer can be divided into the intrinsic and extrinsic whether the light medium in the sensor gage is optical fiber or air. Intrinsic sensors have serious drawbacks such as the beating and drifting of signal. However, there are no handicaps like above for extrinsic sensors. In this study, EFPI sensor was used as shown in Fig. 1.

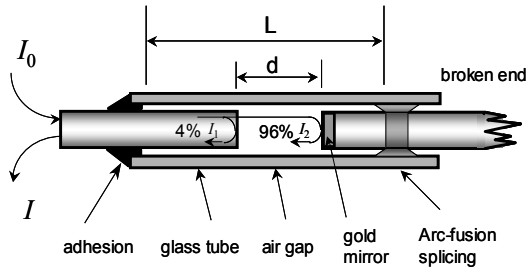

Fig. 1. Schematic diagram of EFPI.

The sensor consist of a hollow glass tube capped over the end of a single-mode input/output fiber. A gold deposited fiber, placed inside the glass tube facing the single-mode fiber, functions as a Fresnel reflector and forms an air gap that acts as a low-finesse EFPI cavity. The first reflection at the glass-air interface acts as the reference reflection signal for the interferometer. The second reflection from the surface of the gold deposited mirror generates the reflected sensing signal. These two form an interferometer and the reflected output intensity can be written as a sinusoidal function.

$$I \propto A(1 + B\cos 2kd) \quad , \; k = 2\pi n_c / \lambda_0 \qquad (1)$$

where A and B are constants, k is the wave propagation number which equals to $2\pi n_c / \lambda_0$, and d is the width of

gap separation. In the equation of k, n_c ($\sqcup$ 1) is the refractive index of core in optical fiber and λ_0 is the wavelength of laser diode in vacuum state, 1305nm. The relation between optical phase and gap separation is $\phi = 2kd$ and L is the gage length of EFPI. Because the fiber core is strain free in the glass tube, using the relation, $\Delta L = \Delta d$, equation of phase shift can be written as follows.

$$\frac{\Delta\phi}{\Delta L} = \frac{4\pi n_c}{\lambda_0} = 0.9629 \times 10^7 \, (rad/m) \qquad (2)$$

Since the light medium of EFPI is air, there is no change in refractive index and sensor has immunity to polarization fading [7]. The signal from EFPI can be converted into the infinitesimal displacement by measuring the cumulative phase shift which is expressed as the intensity variation. From relation between phase-shift and displacement, equation (2), equation of displacement can be evaluated as following.

$$\delta = \Delta L = 0.1039 \times 10^{-6} \times \Delta\phi(m) \qquad (3)$$

Therefore the frequency characteristics of output signal shows the equal dynamic peculiarities of infinitesimal displacement of the sensor.

2.2. Absolute EFPI for strain measurement

The shape of AEFPI sensor is identical to that of EFPI sensor in Figure 1. But it utilizes the concept of white light interferometry in which a broadband source is employed instead of the laser diode. The use of AEFPI system can overcome the limitations of EFPI system such as the non-linearity in the output signal, difficulty in distinction of direction of strain, and requirement of complex fringe counting technique [2]. The signal processing is performed using the computer followed by an optical spectrum analyzer(OSA) in real-time.

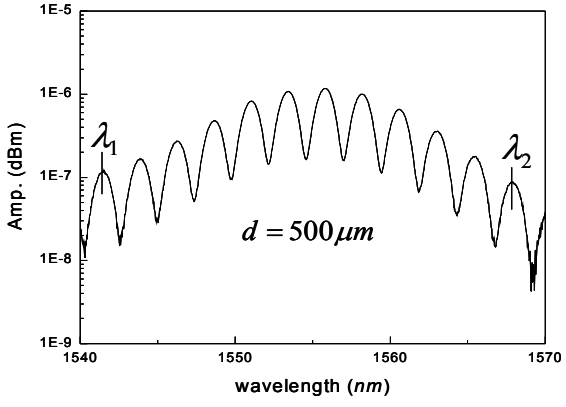

Fig. 2. Typical output of the AEFPI system.

Figure 2 shows the typical AEFPI signal acquired by OSA. Two wavelength λ_1 and λ_2 are determined from the OSA and signal processing program determines the gap separation d unambiguously using the following equation [8].

$$d_i = \frac{m\lambda_1\lambda_2}{2(\lambda_2 - \lambda_1)} \, , (i = 0,\ 1,\ 2...) \qquad (4)$$

where λ_1 and λ_2 are two wavelengths that are $2m\pi$ out of phase and m is an integer. The i is the number of measuring instant, and in case of initial state, $i=0$. If the sensor has a gage length of L, the applied strain can be expressed as

$$\varepsilon = \frac{d_n - d_0}{L} = \frac{\Delta d}{L} \qquad (5)$$

where Δd is the change of gap separation, and d_n, d_0 are the final and initial gap lengths, respectively. The thin deposition of metal such as gold or aluminum on the ends of the fibers enclosing the cavity increases the interface reflectivity and enhances the finesse of the cavity and sensitivity of the sensor. The finesse, F, is the parameter used to characterize Fabry-Perot cavities[2]. In this work, we deposited the gold on the second reflecting fiber end to increase the finesse of the sensor.

3. SIGNAL PROCESSING FOR FAILURE DETECTION

3.1. Short time Fourier transform

In many information processing systems, it is desirable to transform the sensor data from its raw time-domain format to the frequency domain, where appropriate spectral analysis and feature extraction can be applied. The most commonly used method is the Fourier transform. Because this transform use the sinusoidal basis functions which are localized in frequency only, it lost the transient feature of signal data. Therefore it is necessary to adopt the time-frequency analysis for diagnostics of transient signal such as damage induced signals. Moreover the time-frequency analysis can be used for damage monitoring of smart structures.

The short-time Fourier transform (STFT) can be a candidate for the time-frequency analysis. The STFT has a short data windows centered at time t. The idea is that local spectral coefficients are obtained which describe the frequency composition of the record being analyzed at time t. The windows is then moved to a new position and the calculation repeated. The STFT of a signal $f(t)$ is defined as follows.

$$STFT(\tau, \omega) = \int_{-\infty}^{+\infty} f(t) g(t-\tau) e^{-i\omega t} dt \qquad (6)$$

The result can be interpreted as the Fourier transform of the signal $f(t)$ windowed by a function $g(t)$ around time τ. But, unfortunately there is a fundamental problem

with this approach. Because two requirements of a short data windows and a narrow bandwidth are irreconcilable, it is impossible to achieve high resolution in time and frequency simultaneously. STFT, however, does not require long computation time compared with other time-frequency analysis, therefore it is applied in the real-time processing for failure detection. In this study hamming window was applied for STFT and LabView® program language and Signal Processing Toolbox of Matlab® were used for signal processing.

3.2. Wavelet transform

In order to overcome the limitation of harmonic analysis in STFT, alternative families of orthogonal basis functions called wavelets are used instead of sines and cosines as the basis functions for decomposing a general signal. The Wavelet Transform(WT), which decomposes a signal into a set of basis functions which are localized both in time and in frequency, is opposed to the sinusoidal basis functions used by the Fourier transform. Each wavelet function in the basis set is a stretched or narrowed version of a prototype wavelet. Wavelet basis functions have the advantage that they are localized with respect to both time and frequency and act as multi-scale bandpass filters when convoluted with the signal data. While the Fourier transform has the ability to isolate specific frequencies in a signal, the WT is capable of revealing aspects of data that other signal analysis techniques miss, such as transient features, trends, breakdown points, discontinuities in higher derivatives and self-similarity. The continuous wavelet transform is defined as follow,

$$CWT_f(a,b) = \frac{1}{\sqrt{a}} \int_{-\infty}^{+\infty} f(t) \Psi^* \left(\frac{t-b}{a} \right) dt \quad (7)$$

where $a \in R$ and $b \in R$ are scale and shift parameters, respectively, and Ψ^* is complex conjugate of wavelet fuction. The equation implies that we measure the similarity between the signal *f(t)* and shifts and scales of an elementary function. In this study, an efficient algorithm, referred as the fast Wavelet transform(FWT), was employed. In the FWT, a signal may be represented by its approximations and details. The approximations are the high-scale, low-frequency components of the signal. The details are the low-scale, high-frequency components. By selecting different dyadic scales, a signal can be broken into many lower-resolution components, referred as the wavelet decomposition tree. WT was applied for post-processing of failure signal to analyze its characteristics. The Wavelet Toolbox of Matlab® was used to process the signal.

4. EXPERIMENTS AND DISCUSSION

4.1. Failure detection of composite laminates

To assess the failure mechanism of structures, it is important to understand the characteristics of failure signals of composite laminates.

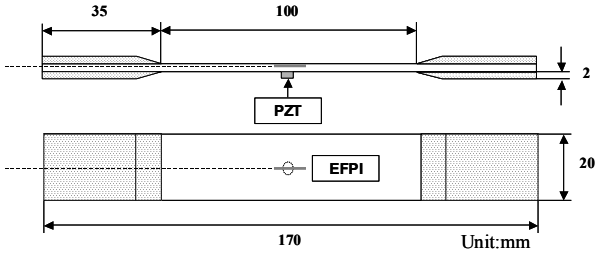

Fig. 3. Configuration of specimen.

In this study, tensile test of graphite/epoxy specimen was performed to obtain the failure signal and time-frequency analysis using STFT and WT was implemented to analyze the signal characteristics. The gage length and gap separation of the EFPI are 9.59 *mm* and 29 μm , respectively. EFPI sensor was embedded in the specimen between the layer of 0° and 90° degree, and on the opposite side PZT was attached to compare the signal response with EFPI. Figure 3 shows the composite specimen for the tensile test. It was made of twenty layer symmetric graphite/epoxy laminates $[0_2/\{0\}/90_{16}/0_2]_T$. The specimen had the dimension of 170 *mm* × 20 *mm* and was clamped to universal test machine(INSTRON, 4482). Material properties of Gr/Ep laminate (HFG CU-125NS) are presented in Table 1 and overall view of experimental setup is shown in Fig. 4.

E_1 (GPa)	E_2 (GPa)	G_{12} (GPa)	ν_{12}	Ply Thickness (mm)
135.4	9.6	4.8	0.31	0.125

Table 1. Material properties of Gr/Ep laminate.

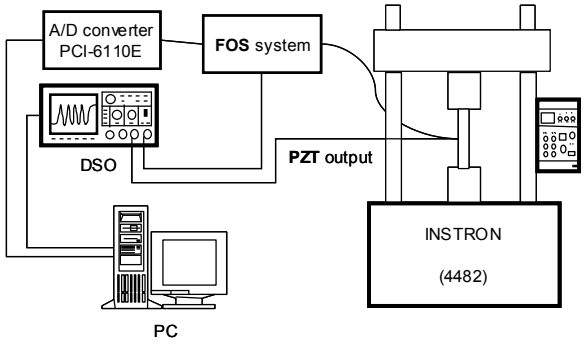

Fig. 4. Overall view of experimental setup.

Though impact or excessive loads are applied on the composite structure, if the damage does not happen, we can only see the sensor signal below the frequency range of 20 *kHz*. But, for the case of structural failure, stress

wave emission induced by matrix cracks or fiber breakages can be observed by examining the 20 *kHz* ~ 200 *kHz* frequency range [9].

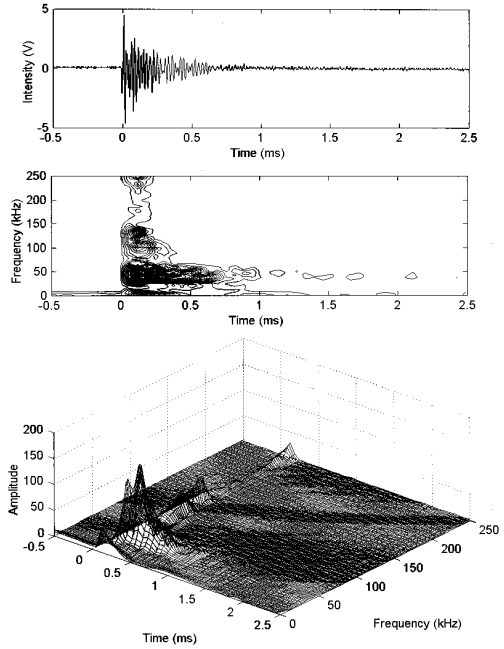

Fig. 5. Matrix crack signal detected by PZT and its STFT.

Figure 5 shows the matrix crack signal detected by PZT sensor and its STFT. In frequency domain, signal could be divided into two region, 20 *kHz* ~ 60 *kHz* and above 60 *kHz*. In the first region, notable peaks with high amplitude were observed around 40 *kHz*, and they lasted about 1 *ms*. And along the frequency region above 60 *kHz*, figures shows that stress waves induced by the generation of matrix crack can be observed by the examining the 60 *kHz* to 250 *kHz* frequency range, which continued about 0.2 *ms* ~ 0.4 *ms*.

Figure 6(a) indicates the EFPI sensor response of matrix cracking signal which is the same as Fig. 5. Comparing with the PZT signal, overall distribution of frequency characteristics of the two signals look alike. However, PZT signal showed more sensitivity around the peaks of 40 *kHz* , EFPI had more uniform and susceptible response over 150 *kHz*.

Figure 6(b) shows the results of the WT decomposition, respectively, at the three kinds of impact using Daubechies 4(*Db*4) wavelet to the level 3. In this figures, '*S*′ represents the raw sensor signal, The details D_1, D_2 and D_3 represent approximately 200 ~ *kHz*, 100 ~ 200 *kHz*, 0 ~ 100 *kHz* signal range respectively from the calculation of approximate frequencies. '*A*′ represents the approximation decomposed by high scaled wavelet function. If the structural failure happen, The generation time of damage is observed in the *D1* ~ *D3*, high frequency component[9]. From the figure, *D1* signal which cover the frequency range over 200 *kHz* continued about 0.2 *ms*. It represents that to detect the moment of failure, the size of the time window should be wider than 0.2 *ms* for the signal processing.

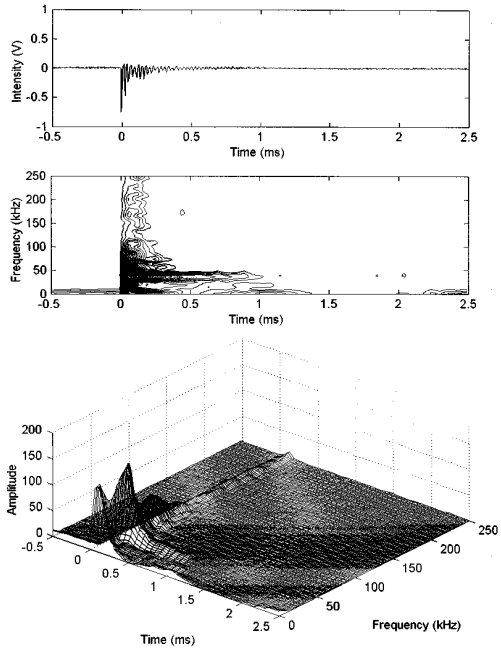

(a) Short Time Fourier Transform.

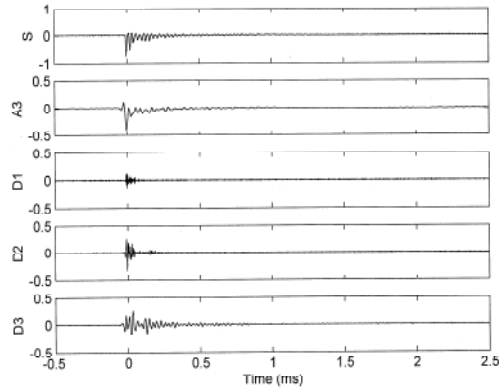

(b) Wavelet Transform.

Fig. 6. Matrix cracking signal detected by EFPI and its STFT & WT.

In the case of fiber breakage, PZT could not sense the signal any more since it separated from the specimen at the moment of damage. But EFPI sensor could detect the fiber breakage signal. Figure 7 shows that the stress wave signals due to fiber breakage are dominantly composed of the detail D_1 and D_3. For D_1, the details of this mode have about three times of amplitude than that of the matrix cracking, and the time duration is much longer. However, the stress wave signals due to matrix cracks are mainly composed of D_2 and D_3.

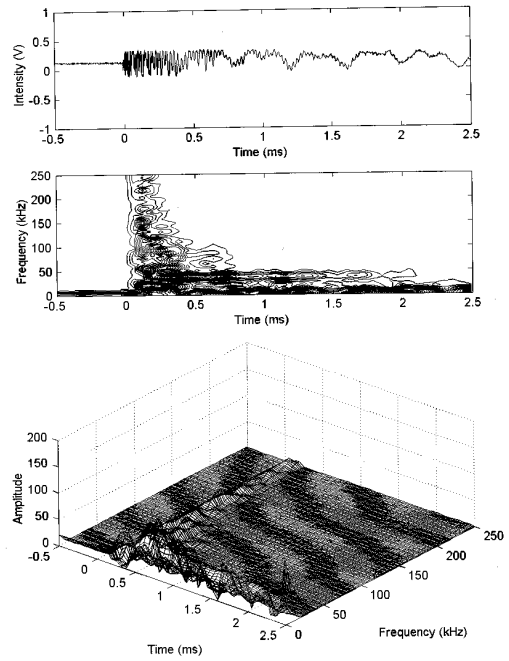

(a) Short Time Fourier Transform.

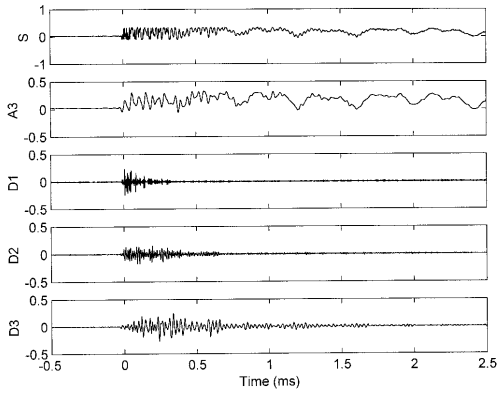

(b) Wavelet Transform.

Fig. 7. Fiber breakage signal detected by EFPI and its STFT & WT.

On the bases of these experimental results, we set the frequency threshold as 25 *kHz* in the failure detection program. Including characteristic frequency of 40 *kHz*, every failure signals over this limit will cause the warning of structural failure by the program.

4.2. Real-time health monitoring

The simultaneous sensing of the strain and failure in composite beams with an embedded fiber optic sensor have been carried out in real-time. To detect the failure signal, EFPI system using laser diode(LD) with 1305 *nm* wavelength was employed. And AEFPI system with ASE broadband source was implemented for the strain measurement. The specimen was made of twenty layer symmetric graphite/epoxy laminates $[0_2/90_{16}/0_2]_T$ and the specimen had the dimension of 170 *mm* × 20 *mm* as the tensile test specimen in Fig. 8. The gage length and gap separation of the EFPI are 10.73 *mm* and 239 μm ,respectively. And, instead of PZT, an electric strain gage was attached on the front surface of it to compare the strain readout with AEFPI. The specimen was clamped to universal test machine(INSTRON,4482) and tensile test was performed.

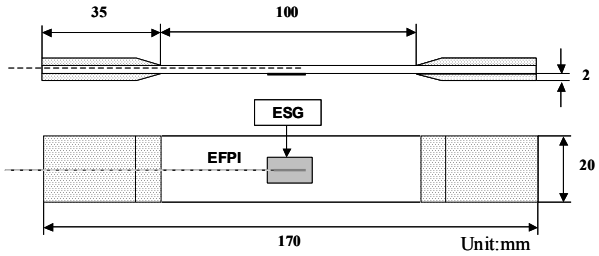

Fig. 8. Configuration of specimen.

To sense the strain and failure simultaneously, two different light source were employed in one EFPI sensor using wavelength division multiplexer. It is the device which can multiplex two (or more) signals of different wavelengths onto the same fiber carrier. The schematic diagram of the fiber optic sensor system is shown in Fig. 9.

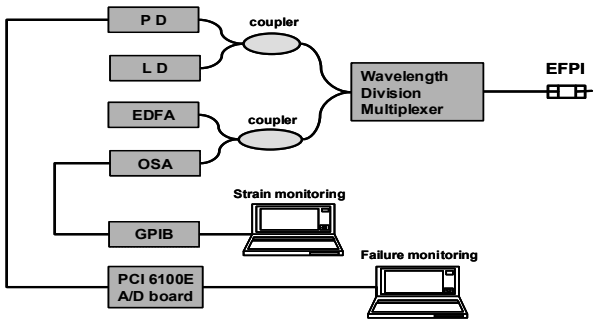

Fig. 9. Optical fiber sensor system for the simultaneous sensing of strain and failure.

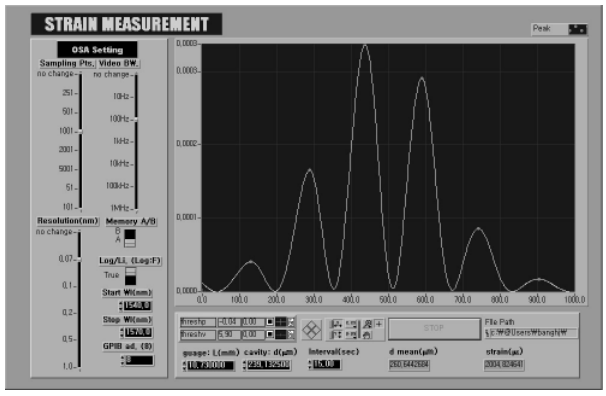

Fig. 10. Real time strain monitoring program.

The strain measurement system consists of ASE source, OSA, and processing computer. OSA is controlled by the program written in LabView® language and transfers the wavelength data to the signal processing computer.

Figure 10. shows the signal processing program for the strain measurement. Wavelength data analyzed from the OSA are processed by this program and the strain values are displayed and recorded in real-time.

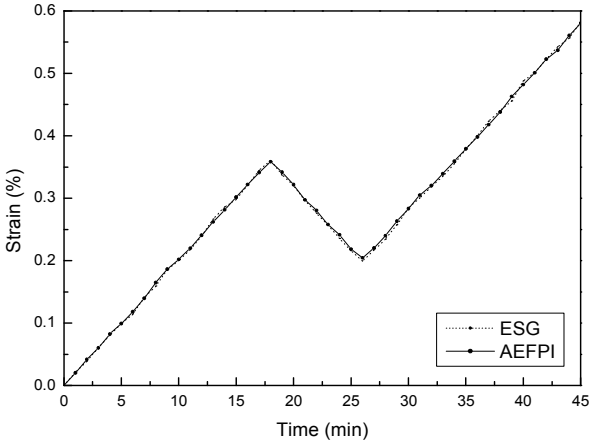

Fig. 11. Experimental result of strain measurement using AEFPI.

At first, tensile loads were increased up to the level before the moment of 0.4% strain when the initial matrix cracks could appear. And the load were released to 0.2 % strain and were increased again to the level of fiber breakage. Figure 11 shows the experimental result of strain data from AEFPI and electric strain gage. The strain measured by AEFPI coincides with the value of electric strain gage. From this result, it is confirmed that AEFPI can be applied to the structural health monitoring system for long time measurement.

Figure 12 indicates the failure signals detected by EFPI sensor. Signals were processed by using real-time STFT. Figure 12(a) shows the matrix crack signal detected on 0.5% strain condition. From this figure, we can observe the peak near 40 *kHz*. In the Fig. 12(b), fiber breakage signal has uniform distribution with high amplitude along the wide frequency range. These results are in accord with the frequency characteristics of the previous result, presented in Fig.6 and Fig. 7.

With AEFPI sensor system, to sense the strain with more accuracy, it is necessary to lengthen the gap separation. But, the wider the gap separation of the sensor, the lower the intensity of failure signal detected by EFPI sensor system. However, in this study, we could detect sensitively the failure signal with the sensor of wide gap separation by using gold deposited reflecting surface shown in Fig. 1.

From the result above, we can confirm that it is possible to develop simultaneous failure detection and strain measurement techniques for health monitoring of composite materials using one EFPI sensor.

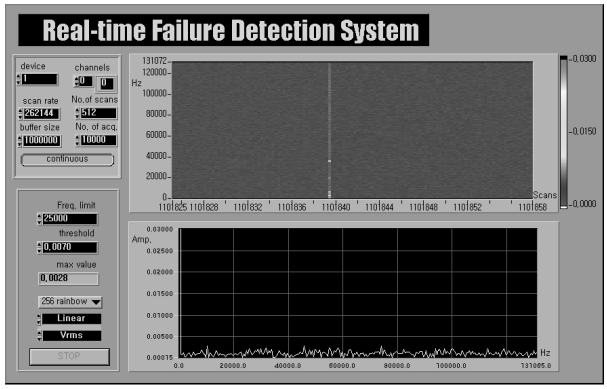

(a) Matrix cracking.

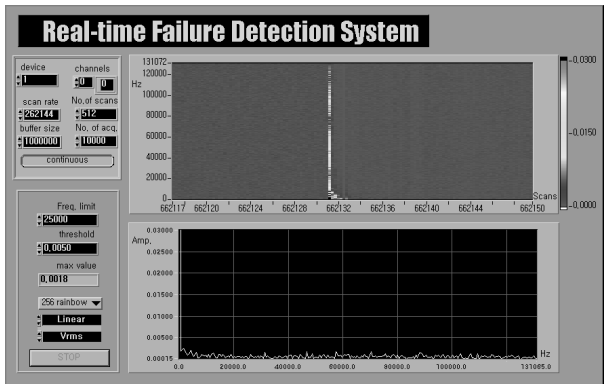

(b) Fiber breakage.

Fig. 12. Failure signals detected by real-time failure detection system.

5. CONCLUSIONS

This paper describes the simultaneous sensing techniques of strain and failure signal. And the frequency characteristics of the failure signal from graphite/epoxy composite laminate are also presented. Tensile tests of composite beams were performed to investigate the signal characteristics of matrix crack and fiber breakage. STFT and WT could quantitatively evaluate the onset of structural failure.

To sense the strain and failure simultaneously, two different light sources were employed in one EFPI sensor using wavelength division multiplexer. In this study, by using gold deposited reflecting surface, we could detect the failure signal with the sensor of wide gap separation which is suitable to strain measurement. The fiber optic sensor system successfully detected the moment of failure and could measure the strain accurately for long period.

Acknowledgment – The authors would like to thank the Agency for Defense Development, Korea, for the financial support of this work.

NOMENCLATURE

n_c : refractive index of fiber core.
λ_0 : wavelength of laser diode in vacuum state.
I : output reflected intensity.
k : wave propagation number ($2\pi n_c / \lambda_0$).
d : gap separation of EFPI.
L : gage length of EFPI.
$\Delta\phi$: cumulative phase-shift in EFPI.

REFERENCES

1. J. S. Sirkis, M. A. Putman, T. A. Berkoff, A. D. Kersey, et al., Proc. Int. Conf. Smart Sensing, Processing, and Instrumentation, Vol.2191 **(**ed. by J. S. Sirkis), SPIE, Orlando (1994) 137.
2. T. A. Tran, J. A. Greene, K. A. Murphy, V. Bhatia, M. B. Sen, and, R. O. Claus, Proc. Int. Conf. Smart Structures and Materials: Industrial and Commercial Applications of Smart Structures Technologies, Vol.2447 (ed. by C. R. Crowe), SPIE, San Diego (1995) 312.
3. K. Liu, S. M. Ferguson, and R. M. Measures, Proc. Int. Conf. Fiber Optic Smart Structures and Skins II, Vol.1170 **(**ed. by E. Udd), SPIE, Boston (1989) 205.
4. J. J. Alcoz, C. E. Lee, and H. F. Taylor, IEEE Transactions on Ultrasonics, Ferroelectrics, and Frequency Control, **37**, No. 4 (1990) 302.
5. K. A. Murphy, C. A. Schmid, T. A. Tran, G. Carman, A. Wang, and R. O. Claus, Proc. Int. Conf. Smart Sensing, Processing, and Instrumentation, Vol.2191 **(**ed. by J. S. Sirkis), SPIE, Orlando (1994) 227.
6. I. B. Kwon, C. G. Kim, and C. S. Hong, Composites Science and Technology, **57** (1997) 1639.
7. J. W. Park, C. Y. Ryu, H. K. Kang, and C. S. Hong, J. of Composite Materials, **34**, No. 19 (2000) 1602.
8. V. Bhatia, M. B. Sen, K. A. Murphy, and R. O. Claus, Electronics Letters, **32**, No. 3 (1996) 247.
9. D. U. Sung, J. H. Oh, C. G. Kim, and C. S. Hong, " J. of Intelligent Material Systems and Structures, **11 (**2000) 180.